Equilibrium-Based Nonhomogeneous Anisotropic Beam Element

Krenk, Steen; Couturier, Philippe

Published in:
A I A A Journal

Link to article, DOI:
10.2514/1.J055884

Publication date:
2017

Document Version
Peer reviewed version

Equilibrium Based Non-homogeneous Anisotropic Beam Element

Steen Krenk[1] and Philippe J. Couturier[2]
Technical University of Denmark, DK-2800, Lyngby, Denmark

The stiffness matrix and the nodal forces associated with distributed loads are obtained for a non-homogeneous anisotropic elastic beam element by use of complementary energy. The element flexibility matrix is obtained by integrating the complementary energy density corresponding to six beam equilibrium states and then inverted and expanded to provide the element stiffness matrix. Distributed element loads are represented via corresponding internal force distributions in local equilibrium with the loads. The element formulation does not depend on assumed shape functions and can in principle include any variation of cross-section properties and load variation provided that these are integrated with sufficient accuracy in the process. The ability to represent variable cross-section properties, coupling from anisotropic materials, and distributed element loads is illustrated by numerical examples.

Nomenclature

A	= cross-section area
a	= half element length
$\mathbf{C}$	= cross-section flexibility matrix
$\mathbf{D}$	= cross-section stiffness matrix
$\mathbf{f}$	= generalized force vector
$\mathbf{f}_j$	= nodal force vector

[1] Professor, Department of Mechanical Engineering, Nils Koppel's Alle, Building 404
[2] Engineer, Siemens Wind Power, Ontario, Canada

f_x, f_y, f_z = force components

$\mathbf{G}$ = element end-point internal force matrix

$\mathbf{g}$ = end-point forces from external load

$\mathbf{H}$ = element flexibility matrix

$\mathbf{h}$ = element deformation from equilibrium states

$\mathbf{K}$ = element stiffness matrix

$\mathbf{M}(s)$ = internal moment vector

$\mathbf{m}_j$ = nodal moment vector

M_x, M_y, M_z = internal moment components

$\mathbf{p}(\xi)$ = external force distribution vector

$\mathbf{Q}(s)$ = internal force vector

Q_x, Q_y, Q_z = internal force components

$\mathbf{q}$ = generalized internal force vector

$\mathbf{r}$ = equivalent nodal force vector

s = length coordinate

$\mathbf{T}(\xi)$ = internal force distribution matrix

$\mathbf{u}$ = generalized displacement vector

u_x, u_y, u_z = displacement components

x, y, z = spatial coordinates

W_s = elastic energy pr. unit length

W_e = element elastic energy

δ = variational increment

$\boldsymbol{\gamma}$ = generalized strain vector

γ_{ij} = normalized flexibility coupling coefficients

$\gamma_x, \gamma_y, \gamma_z$ = generalized strain components

$\boldsymbol{\varphi}$ = rotation vector

$\varphi_x, \varphi_y, \varphi_z$ = rotation components

$\boldsymbol{\kappa}$ = curvature vector

$\kappa_x, \kappa_y, \kappa_z$ = curvature components

ξ = normalized length coordinate

ξ_* = normalized concentrated load location

Subscripts

o = center section value

A = cross-section reference point

j = node number

x, y, z = coordinate component index

Superscripts

$\sim$ = equilibrium force distribution

$*$ = generalized concentrated load

I. Introduction

Beam elements constitute an essential part of many forms of engineering analysis, e.g. for representing beams and columns of civil engineering and aerospace structures, offshore steel structures, and recently large scale composite wind turbine blades. In each case it is desirable to use beam elements that represent a suitable part of the structure, and thus beam elements that permit varying and fully coupled beam properties as well as distributed loads are of considerable interest. The classical formulation of beam elements, still in extensive use, is based on displacement shape functions, and the corresponding internal forces are then obtained by multiplication with the appropriate stiffness parameters. Apart from simple beams with constant properties along the beam axis this typically leads to complications, e.g. in relation to variable cross-section properties, shear deformation, coupling effects associated with the use of composites etc. While e.g. the shear force is well defined the corresponding equivalent shear strain of a cross-section is less clearly defined, and also the possible variation of the position of elastic and shear center along the beam, or indeed the absence of the traditional torsion-flexure uncoupling via a shear center, complicates kinemat-

ically based formulations. Additionally, variable stiffness along a beam element will influence the representation of distributed loads in the form of equivalent nodal loads.

Within linear elastic beam theory most of the indicated restrictions for displacement based formulations can be alleviated by changing to a complementary energy formulation in terms of suitable sets of internal forces. Within the general framework of finite elements the use of complementary energy formulations is limited by the need for a suitable set of internal equilibrium force distributions, see e.g. [1]. For two- and three-dimensional elements this complicates the formulation, and mixed energy principles have been developed. However, for beams suitable internal force equilibrium distributions are readily available, and very compact and versatile formulations can be obtained. A direct and simple solution for a beam in plane bending was obtained directly from elementary statics by Livesley [2]. A complementary energy formulation was obtained for the Bernoulli beam element with variable cross section and the similar Timoshenko by Friedman and Kosmatka [3, 4], and a more general formulation combining shear flexibility, element curvature and distributed loads was presented by Krenk [5]. This formulation was developed for arches with variable cross section in [6] and for distributed loads in [7]. The flexibility formulation has also been used in a large deformation context as part of a co-rotational beam formulation, see e.g. [8].

Common to the papers just mentioned is the assumption of symmetry, leading to one or two-dimensional problems. A central point of the present paper is the development of a beam element with varying non-symmetric cross-sections and general coupling of the various deformation modes via anisotropic material properties. This extension requires representation of general cross-section properties in the form of a cross-section stiffness or flexibility matrix. This can be obtained in a simple way by a two-dimensional representation of the classic beam deformation modes including torsion and shear warping in terms of isoparametric elements [9]. A more detailed description, which in principle condenses the three-dimensional behavior into the cross-section plane, is the so-called Variational Asymptotic Sectional Beam Analysis (VABS) proposed by Hodges and co-workers in [10], and described in more detail in [11] with further developments in [12]. An alternative procedure was developed by Giavotto et al. [13, 14], in which a beam with constant cross-section representing a cross-section of the original beam is analyzed by a 2D or 3D eigenvalue technique, where the

non-decaying deformation modes are extracted and associated with bending, shear, extension and torsion. The technique goes by the name of Anisotropic Beam Analysis (ANBA). Further developments of the associated eigenmode technique have been presented in [15] and [16]. Closer associated with the present paper is a related method, in which the cross-section flexibility properties associated with the non-decaying beam modes are extracted directly from an equivalent prismatic beam by imposing a set of six representative displacement modes [17, 18].

The present paper develops a beam element for variable cross-sections with general anisotropy, and derives specific formulas for the representation of internally distributed loads by equivalent nodal forces. The basic notation and definition of the section properties are introduced in section II. The following theory is divided into two parts. First, the element stiffness matrix is derived from the elementary concept of complementary energy for a beam without distributed loads in section III. The absence of external distributed loads makes this part quite elementary. In section IV the theory is extended to include distributed loads via a corresponding distribution of the internal forces. A proper complementary energy functional is introduced, and elimination of the parameters of the homogeneous internal force distributions then identifies the equivalent nodal forces of the element. Finally, section V gives examples illustrating the effect of anisotropic coupling of the displacement modes and the effect of stiffness variation on the nodal forces, and furthermore combines the effects in the analysis of a realistic wind turbine blade.

II. Definition of General Section Properties

Consider a straight beam, and introduce a coordinate system with the z-axis acting as beam axis, while the cross-sections are parallel with the xy-plane. The internal force vector $\mathbf{Q}(z) = [\,Q_x(z), Q_y(z), Q_z(z)]^T$ at a cross-section defined by z is defined in terms of the stresses on the cross-section $[\,\sigma_{zx}, \sigma_{zy}, \sigma_{zz}]$ as

$$Q_x = \int_A \sigma_{zx}\, dA \quad , \quad Q_y = \int_A \sigma_{zy}\, dA \quad , \quad Q_z = \int_A \sigma_{zz}\, dA \tag{1}$$

In theories for homogeneous prismatic isotropic beams the combined problems of bending and extension are usually referred to the elastic center, while the torsion and shear problems are referred to the center of twist. The resulting relations can then be transformed into a common point of

reference. In the present formulation the deformation modes can be coupled, and no assumptions about particular characteristic points in the cross-section are introduced. Assuming a common point of reference A with coordinates (x_A, y_A) in the cross-section the moment vector $\mathbf{M}(z) = [\, M_x(z), M_y(z), M_z(z)]^T$ at a cross-section at x is defined by the two bending moments

$$M_x \,=\, \int_A (y - y_A)\sigma_{xx}\; dA \quad , \quad M_y \,=\, -\int_A (x - x_A)\sigma_{xx}\; dA \tag{2}$$

and the torsion moment

$$M_z \,=\, \int_A [(x - x_A)\sigma_{zy} - (y - y_A)\sigma_{zx}]\; dA \tag{3}$$

The different sign on the bending moment components is due to the vector format of the bending moments. The internal force and moment components are illustrated in Fig. 1b. By these definitions zero moment corresponds to the force acting at the reference point A.

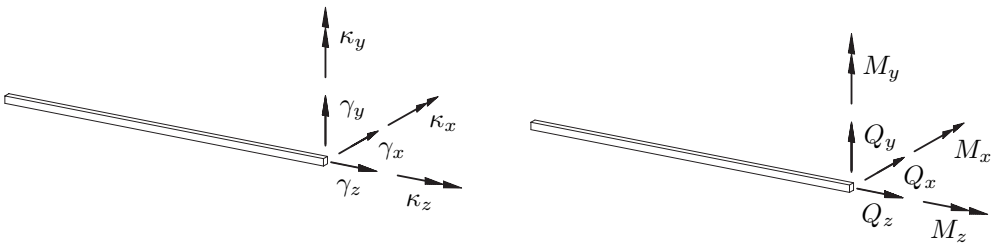

Fig. 1 a) Generalized strains $\boldsymbol{\gamma}(z)$ and curvatures $\boldsymbol{\kappa}(z)$, b) Internal forces $\mathbf{Q}(z)$ and moments $\mathbf{M}(z)$.

It is convenient to collect the six generalized internal force components in the vector $\mathbf{q}(z) = [\, Q_x(z), Q_y(z), Q_z(z), M_x(z), M_y(z), M_z(z)]^T$. In elastic beam theory the deformations associated with the generalized internal forces $\mathbf{q}(z)$ are described in terms of a generalized strain vector $\boldsymbol{\gamma}(z) = [\, \gamma_x(z), \gamma_y(z), \gamma_z(z), \kappa_x(z), \kappa_y(z), \kappa_z(z)]^T$. The components γ_x and γ_y are generalized shear strains, while γ_z is the axial strain of the beam. Similarly, κ_x and κ_y are the components of bending curvature, while κ_z is the rate of twist. The generalized strain and curvature components are defined such that they are conjugate to the internal force and moment components with respect to energy. Thus, the elastic energy per unit length is given as

$$W_s \,=\, \tfrac{1}{2}\boldsymbol{\gamma}^T\mathbf{q} \tag{4}$$

For linear elastic beams there is a linear relation between the generalized internal forces contained in the vector $\mathbf{q}$ and the conjugate generalized strain-curvature vector $\boldsymbol{\gamma}$. This relation can be written either in stiffness format as

$$\mathbf{q} = \mathbf{D}\,\boldsymbol{\gamma} \tag{5}$$

or in the inverse flexibility, or compliance, format

$$\boldsymbol{\gamma} = \mathbf{C}\,\mathbf{q} \tag{6}$$

In these relations $\mathbf{D}$ is the cross-section stiffness matrix, and $\mathbf{C} = \mathbf{D}^{-1}$ is the cross-section flexibility matrix. In general they are both six by six symmetric non-negative definite matrices and may depend on the axial coordinate z. Thus, a general formulation, permitting e.g. anisotropic and inhomogeneous materials, may require up to 21 stiffness or flexibility parameters to describe the deformation properties of a thin slice of the beam.

In classic beam theory without shear flexibility, the shear strain components γ_y and γ_z vanish. This implies that the second and third row and column of the cross-section flexibility matrix $\mathbf{C}$ vanish, and the cross-section stiffness matrix $\mathbf{D}$ becomes singular. In this case a reduced format for the cross section properties can be used. However, in the present formulation the cross-section flexibility matrix $\mathbf{C}$ is used as basis, and no modification is necessary.

The energy per unit length of the beam can be expressed either in terms of the cross-section stiffness matrix $\mathbf{D}$ or the cross-section flexibility matrix $\mathbf{C}$ as

$$W_s = \tfrac{1}{2}\boldsymbol{\gamma}^T\mathbf{D}\,\boldsymbol{\gamma} = \tfrac{1}{2}\mathbf{q}^T\mathbf{C}\mathbf{q} \tag{7}$$

The stiffness matrix of a beam element can be developed from either of these forms. In the first case the distribution of the strains and curvatures $\boldsymbol{\gamma}(z)$ along the beam is required, while in the second case it is the distribution of the internal forces and moments $\mathbf{q}(z)$ that is required. While the distribution of strain and curvature along the element depend on the stiffness properties of the element, the distribution of the internal forces and moments is determined directly by statics. This leads to a simple and general procedure for the stiffness matrix of fairly general beam elements based on flexibility, [5]. The following derivation is based on the flexibility approach. First, the stiffness

matrix of the element is derived, and then the appropriate formulae for representing distributed loads are obtained.

III. Beam Element Stiffness Matrix

The stiffness matrix of a beam element accommodating linear bending and constant extension and torsion has six degrees of freedom at each of its two end nodes as shown in Fig. 2a. The nodal displacements are conveniently organized in a 12 component generalized displacement vector $\mathbf{u}^T = [\,\mathbf{u}_1^T, \boldsymbol{\varphi}_1^T, \mathbf{u}_2^T, \boldsymbol{\varphi}_2^T]$, where $\mathbf{u}_j = [\,u_x, u_y, u_z]_j^T$ and $\boldsymbol{\varphi}_j = [\,\varphi_x, \varphi_y, \varphi_z]_j^T$ denote the displacement and rotation, respectively, at node $j = 1, 2$. The corresponding generalized nodal forces are shown in Fig. 2b and collected in the 12 component generalized force vector $\mathbf{f}^T = [\,\mathbf{f}_1^T, \mathbf{m}_1^T, \mathbf{f}_2^T, \mathbf{m}_2^T]$ illustrated in Fig. 2b, with nodal forces and moments represented by $\mathbf{f}_j = [\,f_x, f_y, f_z]_j^T$ and $\mathbf{m}_j = [\,m_x, m_y, m_z]_j^T$, respectively.

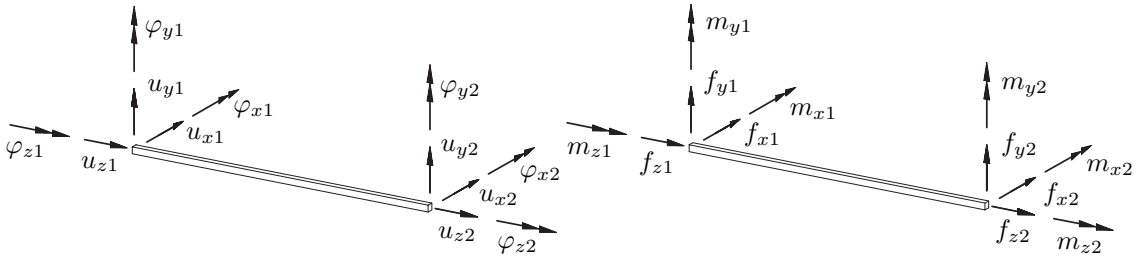

Fig. 2 a) Element displacements $\mathbf{u}_j$ and rotations $\boldsymbol{\varphi}_j$, b) Element forces $\mathbf{f}_j$ and moments $\mathbf{m}_j$.

A. Local deformation modes

The beam element shown in Fig. 2 has 12 degrees of freedom. Of these 6 describe rigid body displacement, while the remaining 6 describe deformation modes of the element. Only the deformation modes contribute to the stiffness of the element, and thus the stiffness matrix of the element can be obtained from the stiffness of these 6 modes, when combined with suitable variable transformations. It is convenient to define the local deformation modes such that they each correspond to a simple set of end loads in equilibrium. There are three modes corresponding to a constant internal force $\mathbf{Q}_0$ in the element, and three modes corresponding to a constant moment $\mathbf{M}_0$ in the element. It is noted that constant shear forces Q_{0x} and Q_{0y} lead to linear anti-symmetric moment variation. Thus, $\mathbf{Q}_0$

is the constant internal force in the beam, while $\mathbf{M}_0$ is the internal moment in the mid-section of the beam.

Let the axial position in the beam element be described by a normalized coordinate ξ on the interval $[-1, 1]$ and let the length of the element be $2a$. The distribution of internal forces is given by the relation

$$\mathbf{q}(\xi) \;=\; \mathbf{T}(\xi)\,\mathbf{q}_0 \tag{8}$$

in terms of the value of the generalized internal force at the center of the beam $\mathbf{q}_0$, and the distribution matrix

$$\mathbf{T}(\xi) \;=\; \begin{bmatrix} 1 & 0 & 0 & 0 & 0 & 0 \\ 0 & 1 & 0 & 0 & 0 & 0 \\ 0 & 0 & 1 & 0 & 0 & 0 \\ 0 & a\xi & 0 & 1 & 0 & 0 \\ -a\xi & 0 & 0 & 0 & 1 & 0 \\ 0 & 0 & 0 & 0 & 0 & 1 \end{bmatrix} \tag{9}$$

It is seen that the distribution matrix is linear in the normalized length coordinate, and that the value of the matrix at the two beam nodes $\mathbf{T}(\pm 1)$ correspond to a unit matrix supplemented by two off-diagonal terms $\pm a$.

B. Flexibility matrix of the equilibrium modes

The flexibility matrix of the equilibrium modes of the element follows from integration of the cross-section flexibility relation (7b) over the element length,

$$W_e \;=\; \int_0^l W_s(s)\; ds \;=\; a \int_{-1}^{1} \tfrac{1}{2}\mathbf{q}(\xi)^T \mathbf{C}(\xi)\,\mathbf{q}(\xi)\, d\xi \tag{10}$$

The generalized internal forces $\mathbf{q}(\xi)$ are represented via the mid-point values $\mathbf{q}$ by (8). The energy of the beam element then takes the form

$$W_e \;=\; \tfrac{1}{2}\mathbf{q}_0^T \mathbf{H}\,\mathbf{q}_0 \tag{11}$$

where the element flexibility matrix $\mathbf{H}$ corresponding to the six equilibrium deformation modes is given by the integral

$$\mathbf{H} = a \int_{-1}^{1} \mathbf{T}(\xi)^T \mathbf{C}(\xi)\, \mathbf{T}(\xi)\, d\xi \tag{12}$$

It is noted that this is an exact expression in which the cross section flexibility is weighted with the linear internal force distribution functions $\mathbf{T}(\xi)$ without involving kinematic assumptions. For a beam of variable cross-section, e.g. a tapered beam or a beam with initial twist, the section flexibility matrix $\mathbf{C}$ is a function of the axial coordinate ξ. It will then be most convenient to evaluate the integral in (12) numerically, either by Gauss quadrature or a combination of mid- and end-point values.

For beam elements with constant section flexibility matrix $\mathbf{C}$ it follows from symmetry that the ξ-terms in $\mathbf{T}(\xi)$ only contribute to the integral via the quadratic terms. There are very few of these, and it is then convenient to carry out the integration in explicit form. The result is the element equilibrium mode flexibility matrix

$$\mathbf{H} = 2a \begin{bmatrix} C_{11} + \frac{1}{3}a^2 C_{55} & C_{12} - \frac{1}{3}a^2 C_{54} & C_{13} & C_{14} & C_{15} & C_{16} \\ C_{21} - \frac{1}{3}a^2 C_{45} & C_{22} + \frac{1}{3}a^2 C_{44} & C_{23} & C_{24} & C_{25} & C_{26} \\ C_{31} & C_{32} & C_{33} & C_{34} & C_{35} & C_{36} \\ C_{41} & C_{42} & C_{43} & C_{44} & C_{45} & C_{46} \\ C_{51} & C_{52} & C_{53} & C_{54} & C_{55} & C_{56} \\ C_{61} & C_{62} & C_{63} & C_{64} & C_{65} & C_{66} \end{bmatrix} \tag{13}$$

It is seen, how the bending parameters $C_{44}, C_{45}, C_{54}, C_{55}$ of the cross-section enter the constant shear modes of the beam element due to their linearly varying bending moment. In the case of beams without shear deformations the first and the second rows and columns in the section flexibility matrix $\mathbf{C}$ vanish, and the bending flexibility terms constitute the only contribution to these rows and columns in the element flexibility matrix. However, the presence of these terms ensures that the element equilibrium mode flexibility matrix $\mathbf{H}$ can be inverted to give the equilibrium mode stiffness matrix $\mathbf{H}^{-1}$. A similar effect occurs in the general expression (12), but is less directly visible.

The equilibrium mode flexibility and stiffness matrices define a set of generalized element strains

$\boldsymbol{\gamma}_0$ by flexibility and stiffness relations similar to (5) and (6) for the cross-section,

$$\boldsymbol{\gamma}_0 \,=\, \mathbf{H}\,\mathbf{q}_0 \;, \qquad \mathbf{q}_0 \,=\, \mathbf{H}^{-1}\,\boldsymbol{\gamma}_0 \tag{14}$$

In contrast to the cross-section relations both the equilibrium mode relations are non-singular also for beams without shear flexibility.

C. From mode flexibility to element stiffness

The relation (8) gives the internal forces in terms of the mid-point values $\mathbf{q}_0$, defining the equilibrium modes. The nodal forces are the internal forces at the nodes with appropriately chosen signs. Therefore the nodal force vector $\mathbf{f}^T = [\,\mathbf{f}_1^T, \mathbf{m}_1^T, \mathbf{f}_2^T, \mathbf{m}_2^T]$ is expressed in terms of the mid-point value of the internal force vector by a relation of the form

$$\mathbf{f} \,=\, \mathbf{G}\,\mathbf{q}_0 \tag{15}$$

where the 12 by 6 matrix $\mathbf{G}$ is expressed by the end point values of the internal force distribution matrix as

$$\mathbf{G} \,=\, \begin{bmatrix} -\mathbf{T}(-1) \\ \\ \mathbf{T}(1) \end{bmatrix} \tag{16}$$

with $\mathbf{T}(\pm 1)$ given by (9).

The relation between the generalized nodal forces $\mathbf{f}$ and the corresponding generalized nodal displacements $\mathbf{u}^T = [\,\mathbf{u}_1^T, \boldsymbol{\varphi}_1^T, \mathbf{u}_2^T, \boldsymbol{\varphi}_2^T]$ follows from use of the principle of virtual work. The virtual work can be expressed both in the 12 component element format and in the 6 component deformation mode format.

$$\delta V \,=\, \delta\mathbf{u}^T\mathbf{f} \,=\, \delta\boldsymbol{\gamma}_0^T\mathbf{q}_0 \tag{17}$$

where $\boldsymbol{\gamma}_0$ denotes the the generalized strains corresponding to the mid-point generalized force vector $\mathbf{q}_0$. When the generalized force components in the 12 component format are represented in terms of their 6 component counterpart by the transformation (16), the following representation of the 6 component deformation measures is obtained,

$$\boldsymbol{\gamma}_0 \,=\, \mathbf{G}^T\mathbf{u} \tag{18}$$

The transformation matrix in the present kinematic strain-displacement relation is the transpose of the transformation matrix in the static external-internal force relation (15).

The stiffness matrix in the 12 component format follows from expressing the energy of the element - first in the 6 component deformation mode format, and then in the 12 component displacement format by use of the transformation (18). In the 6 component format the energy is

$$W_e = \tfrac{1}{2}\boldsymbol{\gamma}_0^T \mathbf{H}^{-1} \boldsymbol{\gamma}_0 \tag{19}$$

where $\mathbf{H}^{-1}$ is the stiffness matrix of the equilibrium mode representation. Substitution of the generalized equilibrium mode strain vector by use of (18) gives

$$W_e = \tfrac{1}{2}\mathbf{u}^T \mathbf{K} \mathbf{u} \tag{20}$$

where the element stiffness matrix $\mathbf{K}$ is

$$\mathbf{K} = \mathbf{G}\,\mathbf{H}^{-1}\,\mathbf{G}^T \tag{21}$$

This transformation generates the 12 by 12 element stiffness matrix $\mathbf{K}$ from the inverse of the 6 by 6 equilibrium mode flexibility matrix $\mathbf{H}$. As already mentioned, the additional terms in the upper left 2 by 2 block of the flexibility matrix $\mathbf{H}$ in (13) ensures the existence of the inverse $\mathbf{H}^{-1}$, also in the case of vanishing shear flexibility.

In the simple case of a homogeneous beam with double symmetry the flexibility matrix (13) is easily evaluated and inverted explicitly, whereby the beam element stiffness matrix (21) including shear flexibility follows directly in closed form, see e.g. [19] Section 3.7.

IV. Representation of distributed load

While the previous section concentrated on the beam element stiffness matrix it is often of interest to provide a correct representation of distributed loads. The detailed distribution of the equivalent nodal loads, used to represent the distributed load, depends on the properties of the element. As the load distribution depends on the element properties along the beam, the equivalent loads constitute a natural part of the theoretical basis of the complementary energy based element.

A. Basic theory

The first step in the formulation of an equilibrium element with distributed load is to identify a set of generalized internal forces that are in equilibrium with the distributed load. These are collected in the six-component vector $\tilde{\mathbf{q}}(z) = [\tilde{Q}_x(z), \tilde{Q}_y(z), \tilde{Q}_z(z), \tilde{M}_x(z), \tilde{M}_y(z), \tilde{M}_z(z)]^T$, and the full distribution of the internal forces then has the form

$$\mathbf{q}(\xi) \,=\, \tilde{\mathbf{q}}(\xi) \,+\, \mathbf{T}(\xi)\,\mathbf{q}_0 \tag{22}$$

It is noted that the selection of the set of internal forces $\tilde{\mathbf{q}}(\xi)$ that keep equilibrium with the external load is not unique, as they may contain any linear combination of the generalized internal force distributions from the homogeneous solutions. This gives a considerable freedom in the specific choice of the distributions in $\tilde{\mathbf{q}}(\xi)$, and it is convenient to choose these as corresponding to simple boundary conditions. The generalized section forces contained in the vector $\mathbf{q}_0$ in (22) correspond to the component values of the additional homogeneous part at the center of the element.

The specific complementary elastic energy corresponding to a unit length of the beam is now given as

$$W_s \,=\, \tfrac{1}{2}\mathbf{q}^T\mathbf{C}\mathbf{q} \,=\, \tfrac{1}{2}\tilde{\mathbf{q}}^T\mathbf{C}\tilde{\mathbf{q}} \,+\, \tilde{\mathbf{q}}^T\mathbf{C}\mathbf{T}\mathbf{q}_0 \,+\, \tfrac{1}{2}\mathbf{q}_0^T\mathbf{T}^T\mathbf{C}\mathbf{T}\mathbf{q}_0 \tag{23}$$

This corresponds to the total complementary energy

$$W_c \,=\, \int_0^l W_s(s)\,ds - \mathbf{u}^T\mathbf{f} \tag{24}$$

The vector $\mathbf{f}$ contains the generalized reaction forces at the ends of the beam, here given as

$$\mathbf{f} \,=\, \mathbf{g} \,+\, \mathbf{G}\,\mathbf{q}_0 \tag{25}$$

with the 12-component vector $\mathbf{g}$ containing the end point values corresponding to the section forces $\tilde{\mathbf{q}}(\xi)$,

$$\mathbf{g} \,=\, \begin{bmatrix} -\tilde{\mathbf{q}}(-1) \\ \\ \tilde{\mathbf{q}}(1) \end{bmatrix} \tag{26}$$

and the 12 by 6 matrix $\mathbf{G}$ defined in (16).

When carrying out the integration, the complementary energy (24) can be expressed in the form

$$W_c \,=\, \tfrac{1}{2}\mathbf{q}_0^T\mathbf{H}\mathbf{q}_0 \,+\, \mathbf{h}^T\mathbf{q}_0 \,+\, h \,-\, \mathbf{u}^T\big(\mathbf{G}\,\mathbf{q}_0 \,+\, \mathbf{g}\big) \tag{27}$$

where the matrix $\mathbf{H}$ is given by (12), the vector $\mathbf{h}$ is defined by

$$\mathbf{h} = a \int_{-1}^{1} \mathbf{T}(\xi)^T \mathbf{C}(\xi)\, \tilde{\mathbf{q}}(\xi)\, d\xi \tag{28}$$

and the scalar h is without importance for the element properties.

The static variables $\mathbf{q}_0$, defining the homogeneous part of the internal forces (22), are determined from the stationarity condition

$$\frac{\partial W_c}{\partial \mathbf{q}_0^T} = \mathbf{H}\mathbf{q}_0 + \mathbf{h} - \mathbf{G}^T\mathbf{u} = \mathbf{0} \tag{29}$$

whereby

$$\mathbf{q}_0 = \mathbf{H}^{-1}\big(\mathbf{G}^T\mathbf{u} - \mathbf{h}\big) \tag{30}$$

Upon substitution of this value, the complementary energy (27) takes the form

$$W_c = -\tfrac{1}{2}\mathbf{u}^T\mathbf{K}\,\mathbf{u} + \mathbf{u}^T\mathbf{r} + \text{const} \tag{31}$$

where $\mathbf{K}$ is the element stiffness matrix (21), while the equivalent nodal forces on the element are given by the vector

$$\mathbf{r} = \mathbf{G}\,\mathbf{H}^{-1}\mathbf{h} - \mathbf{g} \tag{32}$$

In this expression the second term is the nodal forces corresponding to the non-homogeneous part of the internal force distribution $\tilde{\mathbf{q}}$, given explicitly by (26), while the first term represents the contribution from the homogeneous part of the internal force distribution activated to satisfy the kinematic boundary conditions of the element. While different choice of equilibrium internal force distributions will influence the end point force component vector $\mathbf{g}$, these differences are absorbed in the first term, making the load vector $\mathbf{r}$ independent of the particular choice of the equilibrium distributions. This is similar to the freedom in selecting a statically determinate system in the force method for beams and frames.

B. Simple internal loads

The equivalent nodal forces $\mathbf{r}$ are determined by (32) via the corresponding distribution of the internal forces $\tilde{\mathbf{q}}(\xi)$, in part by using the end point values to define the vector $\mathbf{g}$, given by (26),

and in part by using the internal force distribution to evaluate the integral $\mathbf{h}$, given by (28). The internal force distributions $\tilde{\mathbf{q}}(\xi)$ must represent equilibrium with the distributed load on the element, but this leaves considerable freedom in the construction of these distributions corresponding to different support conditions at the nodes. Here, a simple but rather general procedure for continuous distributed loads is described. Let the vector $\mathbf{p}(\xi) = [\,p_x(\xi), p_y(\xi), p_z(\xi), m_x(\xi), m_y(\xi), m_z(\xi)\,]^T$ represent the the components of distributed force and moment components over the beam element, where $-1 \le \xi \le 1$ is the non-dimensional coordinate introduced in connection with the homogeneous internal force distribution (8). It is then easily verified that the beam equilibrium equations are satisfied by an internal force distribution vector determined by

$$\tilde{\mathbf{q}}(\xi) \;=\; -a \int_{\xi_0}^{\xi} \mathbf{T}(\xi - \tilde{\xi})\, \mathbf{p}(\tilde{\xi})\, d\tilde{\xi}\,, \tag{33}$$

where $\mathbf{T}(\xi)$ is the interpolation matrix introduced in (9). The lower limit ξ_0 in the integral is arbitrary. The factor a in front of the integral is due to the fact that the distributed load corresponds to $\mathbf{p}\, dz = a\mathbf{p}\, d\xi$.

The expression (33) is easily integrated numerically, but explicit results are easily obtained for the case of power function distributions of the form

$$\mathbf{p}(\xi) \;=\; \xi^{n-1}[\,p_x, p_y, p_z, m_x, m_y, m_z\,]_n^T \;=\; \xi^{n-1}\mathbf{p}_n \tag{34}$$

for $n = 1, 2, \cdots$. When introducing this load density distribution into (33) with lower limit $\xi_0 = 0$, the resulting internal force distribution can be arranged in the compact form

$$\tilde{\mathbf{q}}_n(\xi) \;=\; -\frac{a}{n}\, \xi^n\, \mathbf{T}\Big(\frac{a\,\xi}{n+1}\Big)\, \mathbf{p}_n\,. \tag{35}$$

The corresponding end point force vector $\mathbf{g}$ follows immediately by (26).

A concentrated load acting at the point described by the non-dimensional coordinate ξ_* is represented as

$$\mathbf{p}(\xi) \;=\; \delta(\xi - \xi_*)[\,P_x^*, P_y^*, P_z^*, M_x^*, M_y^*, M_z^*\,]^T \;=\; \delta(\xi - \xi_*)\mathbf{p}_* \tag{36}$$

where $\delta(\xi)d\xi = \delta(z)dz$ is the the distributed load described by the Dirac delta function. In the present case it is convenient to take the lower limit in the generic formula (33) as one of the end-points, corresponding to $\xi_0 = \pm 1$. When using the left end of the element, $\xi_0 = -1$, the integral

takes the form

$$\tilde{\mathbf{q}}(\xi) \,=\, -\int_{-1}^{\xi} \mathbf{T}(\xi-\tilde{\xi})\,\delta(\tilde{\xi}-\xi_*)\,\mathbf{p}_*\,d\tilde{\xi} \,=\, \begin{cases} \mathbf{0}\,, & \xi < \xi_*\,, \\ -\mathbf{T}(\xi-\xi_*)\,\mathbf{p}_*\,, & \xi \geq \xi_*\,. \end{cases} \tag{37}$$

While all internal force components include a piecewise constant contribution, the bending moments also contain a piecewise linear contribution from the corresponding transverse force. The present choice of the left end point as the lower integration limit corresponds to an end without supports, and the internal force distribution corresponds to a beam that is built in at the right end. The corresponding end point force vector $\mathbf{g}$ follows from (26) in the form

$$\mathbf{g} \,=\, \begin{bmatrix} \mathbf{0} \\ -\mathbf{T}(1-\xi_*)\,\mathbf{p}_* \end{bmatrix}. \tag{38}$$

Alternatively, the internal force distribution can be found for a cantilever beam built in at the left end by selecting the integration limit as $\xi_0 = 1$.

In the discussion of element loads their distribution along the beam has been assumed known, thereby enabling the construction of equilibrium internal force distributions. In the case of displacement-dependent loads, such as e.g. follower forces, the distributed load depends on the displacement distribution within the element. However, while the distribution of internal forces depends on the displacements up to second order derivatives, the load dependence will usually be via the angle or first order displacement derivative, and therefore be less sensitive to the details of the displacement distribution. Thus, an assumed displacement distribution in terms of the classic linear-cubic interpolation format will typically lead to an acceptable representation of displacement dependent loads.

V. Examples

The equilibrium formulation and its capacity to include anisotropy and distributed loads for non-homogeneous beam elements are illustrated by four examples: a homogeneous box beam with bend-twist coupling introduced via composite wall properties carrying a concentrated end load or a distributed load, a linearly tapered beam with solid circular cross-section, and finally the analysis of a realistic modern wind turbine blade.

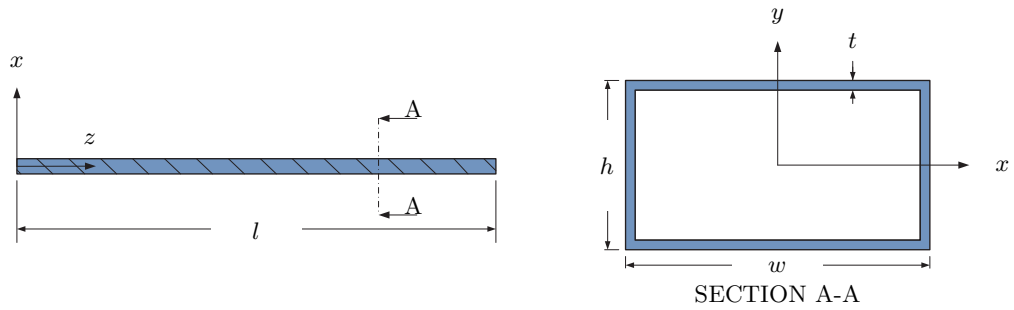

Fig. 3 Composite thin-walled box beam.

A. Composite box beam with end load

This example concerns the analysis of a composite box beam, shown in Fig. 3, that exhibits bend-twist coupling via the use of fibers forming an angle with the beam axis. The particular beam properties were introduced by Stample and Lee [22] and investigated experimentally by Chandra et al. [20] for three different fiber orientations. The beam has a length of $l = 762\,\text{mm}$ (30 in.), a width of $w = 24.2\,\text{mm}$ (0.953 in.), a height of $h = 13.6\,\text{mm}$ (0.537 in.) and a uniform wall thickness of $t = 0.76\,\text{mm}$ (0.030 in.). The walls of the section are made up of six laminas with $E_i = 142.0\,\text{GPa}$ (20.59E+06 psi), $E_j = E_k = 9.79\,\text{GPa}$ (1.42E+06 psi), $G_{ij} = G_{ik} = 6.00\,\text{GPa}$ (8.7E+05 psi), $G_{jk} = 4.80\,\text{GPa}$ (6.96E+05 psi) and $\nu_{ij} = \nu_{ik} = 0.42$, $\nu_{jk} = 0.02$ where i denotes the fiber direction, j the transverse direction, and k the direction normal to the plane of the lamina. The fiber orientation angle α is defined as the angle between the longitudinal axis z and the fiber direction, with a positive angle corresponding to a right-hand helix. The layup sequence for the top and bottom walls are $(-\alpha)_6$ and $(\alpha)_6$, respectively, and for left and right walls are $(-\alpha, \alpha)_3$ and $(\alpha, -\alpha)_3$, respectively. The layup sequence is defined from the innermost to the outermost layers. The $-\alpha$ fiber angle of the top wall can be seen in Fig. 3.

The cross-section stiffness parameters for the three different fiber orientations $\alpha = 15°$, $30°$, and $45°$ were obtained by the computer code CrossFlex based on the representation of the cross-section as a slice with the thickness of a single element with cubic displacement interpolation, and extracting the cross-section parameters by use of complementary energy, [18]. Each of the six lamina were represented by a layer of elements and 50 segments were used in the circumferential direction for a total of 300 solid elements. A modified cross-section analysis in terms of layered elements would

lead to a substantially reduced model size, but this aspect is outside the scope of the present paper. The result of the cross-section analysis is the full six by six symmetric cross-section stiffness matrix. The parameters in the stiffness matrix are listed in Table 1, in which the off-diagonal elements are given in terms of the non-dimensional coefficients

$$\gamma_{ij} = \frac{D_{ij}}{\sqrt{D_{ii}\, D_{jj}}}. \tag{39}$$

representing coupling in the normalized form $-1 < \gamma_{ij} < 1$, with ± 1 representing the maximum possible coupling. All three configurations exhibit a large bend-twist coupling γ_{13} and extension-shear coupling γ_{46}, where the beam with $\alpha = 30^\circ$ exhibits the largest coupling.

The static behaviour of the composite box beam when clamped at one end and loaded with a transverse force at the free end has been investigated experimentally by Chandra et al. [20] for the three different fiber orientations. The measured twist and the bending slope at the middle of the beam due to a tip torque are shown in Fig. 4 and Fig. 5, respectively, together with results obtained from the present model using a single beam element with the cross-section stiffness parameters given in Table 1. These results are compared with results obtained by Smith and Chopra [21] using an analytical model, with results from a finite element approach developed by Stample and

Table 1 Cross-section stiffness properties of box section.

	Units	$\alpha = 15^\circ$	$\alpha = 30^\circ$	$\alpha = 45^\circ$
GA_1	[N]	3.94E+05	5.37E+05	4.12E+05
GA_2	[N]	1.76E+05	3.02E+05	3.08E+05
EA	[N]	6.11E+06	2.80E+06	1.14E+06
EI_1	[Nm^2]	1.75E+02	8.20E+01	3.53E+01
EI_2	[Nm^2]	4.10E+02	1.83E+02	8.09E+01
GJ	[Nm^2]	4.98E+01	7.53E+01	6.18E+01
γ_{12}		1.42E−03	1.98E−03	1.48E−03
γ_{13}		−5.28E−01	−5.61E−01	−4.19E−01
γ_{23}		−6.62E−04	−7.94E−04	−3.21E−05
γ_{45}		−4.02E−03	−4.19E−03	−2.07E−03
γ_{46}		5.55E−01	6.14E−01	4.62E−01
γ_{56}		−7.15E−03	−7.22E−03	−5.05E−03

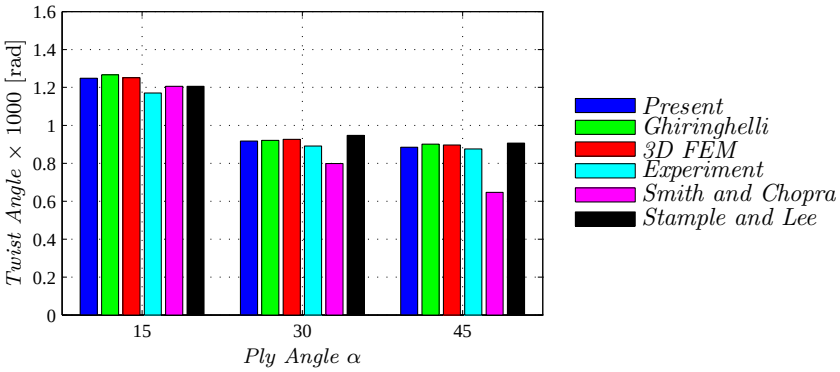

Fig. 4 Twist at mid span of box beam under tip torque of 0.113 Nm [1 lb in.].

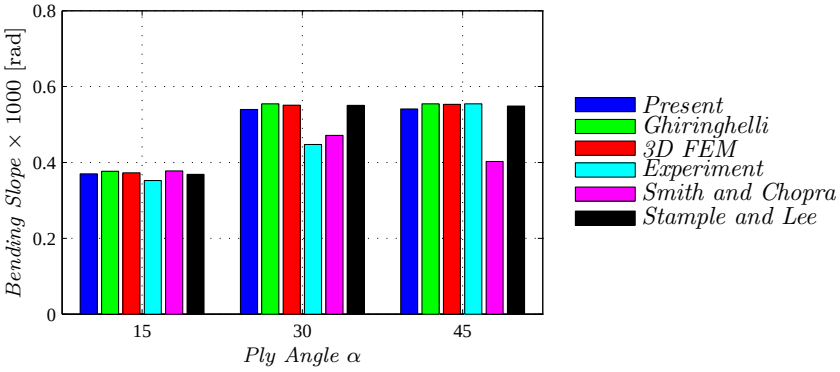

Fig. 5 Bending slope at mid span of box beam under tip torque of 0.113 Nm [1 lb in.].

Lee [22], and results obtained by Ghiringhelli [23] using a complementary energy based beam model with cross-section properties using the 2D formulation in [14], as well as a quite detailed 3D finite element model.

For all three fiber configurations the results obtained using the present beam model agree well with the 3D finite element model, the finite element beam model developed by Ghiringhelli, as well as with the beam model developed by Stample and Lee. Good agreement is also obtained with the experimental results with the exception of the bending slope for the beam with $\alpha = 30°$. Ghiringhelli [23] offers an explanation for this discrepancy by pointing out that the experimental result at $\alpha = 30°$ deviates from the regular curve found by evaluating the bending slope at every 5° fiber angle.

Table 2 Box beam tip deflection from uniformly distributed torque $p_3 = 1/l$ N/m.

Load vector	N_{elem}	u_x [m]	u_y [m]	φ_z [rad]
Consistent	1	3.79E−04	6.55E−02	1.10E−02
Equivalent	1	2.84E−04	4.91E−02	1.10E−02
Equivalent	6	3.76E−04	6.50E−02	1.10E−02
Equivalent	30	3.79E−04	6.55E−02	1.10E−02

B. Composite box beam with distributed load

Consider the cantilever box beam with $\alpha = 15^\circ$ subjected to a uniformly distributed torque with intensity $m_z = 1/l$ N. A distributed torque may arise from pitching moments on airfoils and from distributed loads with an offset from the shear center of the beam. The element nodal load vector for such a prismatic beam with bend-twist coupling subject to a distributed torque can be obtained from (32) as

$$\mathbf{r} = m_z \, [-\psi_1, \, \psi_2, \, 0, \, -a\psi_2, \, -a\psi_1, \, a, \, \psi_1, \, -\psi_2, \, 0, \, -a\psi_2, \, -a\psi_1, \, a \,]^T \ , \tag{40}$$

where the coefficients

$$\psi_1 = \frac{a^2 \, C_{56}}{a^2 \, C_{55} + 3 \, C_{11}} \ , \quad \psi_2 = \frac{a^2 \, C_{46}}{a^2 \, C_{44} + 3 \, C_{22}} \ . \tag{41}$$

represent the effect of bend-twist coupling on the distribution of the nodal loads. Omission of these terms, by setting $\psi_1 = \psi_2 = 0$, corresponds to classic statically equivalent nodal loads.

The tip displacements of the beam from the distributed torque using the consistent load vector (40) and a reduced form with $\psi_1 = \psi_2 = 0$ are presented in Table 2. The tip displacements u_x and u_y calculated using the reduced load vector converge to the correct values, obtained using a single element with the consistent nodal loads. Moreover, the models with one and six elements using the reduced load vector under-predict the in-plane displacements by 25% and 0.7%, respectively. The tip rotation in this example is identical between all models as it is unaffected by the type of load vector used. Using the statically equivalent loads, $\psi_1 = \psi_2 = 0$, introduces an error that decreases with element size, while the consistent representation of the nodal loads permits full accuracy using a single element.

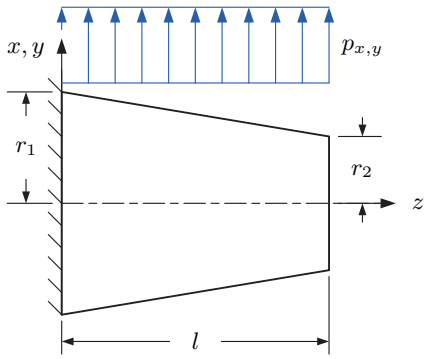

Fig. 6 Tapered beam with circular cross-section and uniform transverse load distribution.

C. Tapered beam with circular solid cross-section

Consider a cantilever beam with solid circular cross-section shown in Fig. 6. The cross-section tapers from radius r_1 to r_2 over the length $l = 2a$. Let the ratio between the end radius be defined by $\beta = r_2/r_1$. The area has as quadratic variation and the moment of inertia has a quartic variation. The analytical solution for the tip deflection $u_{x,y}(l)$ from a uniformly distributed transverse load $p_{x,y}$ can be obtained using the principle of virtual work with $\beta < 1$,

$$u_{x,y}(l) = \frac{p_{x,y}\, l^2}{\pi} \left[\frac{l^2 \left(6 \ln(1/\beta) + 2\beta^3 - 9\beta^2 + 18\,\beta - 11 \right)}{3E\, r_1^4 (1-\beta)^4} + \frac{\beta - 1 + \ln(1/\beta)}{kG\, r_1^2 (1-\beta)^2} \right] , \tag{42}$$

where E, G, and k are the modulus of elasticity, the shear modulus, and the shear correction factor, respectively. The beam is statically determinate, and thus the tip displacement consists of two additive contributions, a contribution from bending flexibility, and a contribution from shear deformation.

The consistent nodal loads for a tapered circular beam element without including the effect of shear flexibility are obtained by integrating (28),

$$\mathbf{r} = [\, p_x f_1,\, p_y f_1,\, 0,\, -p_y m_1,\, p_x m_1,\, 0,\, p_x f_2,\, p_y f_2,\, 0,\, p_y m_2,\, -p_x m_2,\, 0 \,]^T , \tag{43}$$

where the parameters f_1 and m_1 corresponding to node 1 are determined as

$$f_1 = 2a\, \frac{1 - \beta + \beta\, \ln(\beta)}{(1-\beta)^2} , \qquad m_1 = 2a^2\, \frac{1 + \beta - 2\,\beta^2 + \beta\,(\beta+2) \ln(\beta)}{(\beta^2 + \beta + 1)\,(1-\beta)^2} . \tag{44}$$

The similar parameters f_2 and m_2 for node 2 are obtained by replacing β with $1/\beta$ in (44). The values of the load distribution parameters in (44) are shown in Fig. 7 as function of the taper ratio β. For a cylindrical beam, $\beta = 1$, the shear force and end moment parameters are equal at both

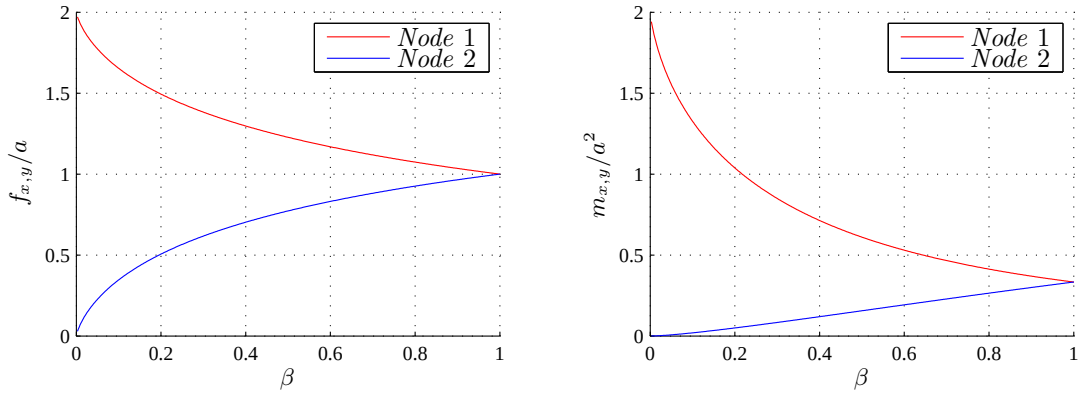

Fig. 7 Nodal force parameters for a uniformly distributed transverse load on tapered element.

nodes with $f_1 = f_2 = a$ and $m_1 = m_2 = a^2/3$. As the beam approaches a perfect cone with $\beta = 0$, all the equivalent nodal loads are shifted to the node with the larger radius with $f_1 = 2a$, $f_2 = 0$ and $m_1 = 2a^2$, $m_2 = 0$.

Consider a specific tapered beam with solid circular cross-section with length $l = 64\,\mathrm{m}$, root diameter $r_1 = 1.2\,\mathrm{m}$ and tip diameter $r_2 = 0.12\,\mathrm{m}$, corresponding to $\beta = 0.1$. The beam is made of an orthotropic material with axial modulus of elasticity $E = 10.0\,\mathrm{GPa}$ and shear modulus $G = 2.0\,\mathrm{GPa}$. The cross-section dimensions and elasticity parameters correspond roughly to the flapwise bending of a wind turbine rotor blade with a bending stiffness ratio of $\beta^4 = 10^{-4}$. The beam is loaded by a uniformly distributed transverse load $p_y = 1.0\,\mathrm{N/m}$.

Table 3 Tapered beam tip deflection from a uniformly distributed load $p_y = 1.0\,\mathbf{N/m}$.

Element	Load Vector	N_{elem}	u_y [mm]	% error
Tapered	shear	1	0.594	0.0
Tapered	no shear	1	0.496	16.4
Tapered	no shear	2	0.561	5.5
Tapered	no shear	4	0.586	1.2
Cylinder	shear	1	1.408	137.3
Cylinder	shear	2	1.057	78.1
Cylinder	shear	4	0.765	28.9
Cylinder	shear	16	0.604	1.8

The tip deflection of the beam when loaded by a distributed load with constant intensity follows from either the full element formulation with stiffness matrix $\mathbf{K}$ from (21) and nodal forces from (32), or the analytical expression (42). The result for a solid cross-section including the effect of shear flexibility with shear correction factor $k = 0.85$ is presented in the first line of Table 3. Any subdivision of the beam using the nodal loads for the conical beam element as given by (32) will recover this result. This result is compared with the deflection calculated by use of the equilibrium element, with the equivalent nodal loads (43) that do not include the effect of shear flexibility. It is seen that while a single element is sufficient to obtain the correct tip deflection if fully integrated, four elements are needed for reducing the error to 1.2 % when the load is distributed according to (43) with load distribution coefficients (44) that do not account for the shear flexibility. Thus, in principle it is necessary for obtaining the full accuracy of the equilibrium element in connection with distributed loads to evaluate the equivalent nodal loads by detailed integration.

The lower part of Table 3 shows the effect of representing the beam in terms of cylindrical elements with radius determined as the radius at the center cross-section. This is a method often used in practice. It is seen that for this kind of approximation 16 elements are needed to reduce the tip deflection error to 1.8 %, demonstrating a considerable gain in accuracy obtained by use of equilibrium based elements.

D. Wind Turbine Blade

The final example concerns the analysis of a 75 m long wind turbine blade currently manufactured by Siemens Wind Power A/S and illustrated in Fig. 8. The blade is constructed using a single web design with the shell and spar cap made of fiberglass-epoxy, while a sandwich core present in the trailing edge walls and tail is made of balsa and foam. The distribution along the blade length of bending stiffness about each of the principal axes of bending normalized with respect to the bending stiffness of the circular root section are shown in Fig. 9a. This gives an illustration of the large cross-section property variations that must be captured when modelling wind turbine blades. It can be seen that for the first half of the blade the bending stiffness in the edgewise direction is typically twice as large as the stiffness in the flapwise direction. The increase in the edgewise bending stiffness

near the root is associated with the transition from a circular to an airfoil cross-section.

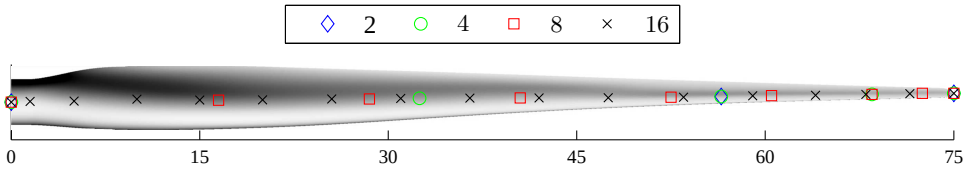

Fig. 8 Rotor blade model discretization.

In the current analysis, the blade is discretized using five different beam element meshes, each with a different number of elements and location of the nodes as shown in Fig. 8. The nodes are positioned along the elastic axis. A fine mesh with 75 elements of equal length has been omitted from the figure for clarity. The node positions for the mesh with two, four and eight elements are optimized to minimize the error of the first four natural frequencies. As expected, the nodes are skewed towards the more compliant outward part of the blade, as shown in Fig. 8. The natural frequencies have been calculated using classic polynomial based shape functions in the evaluation of the mass matrix. This leads to satisfactory results, because the mass matrix integrals do not involve derivatives of the shape functions and is therefore less sensitive to their detailed representation. Furthermore, the major contribution to the inertia comes from the rigid-body motion of the elements, that is not influenced by the local deformation.

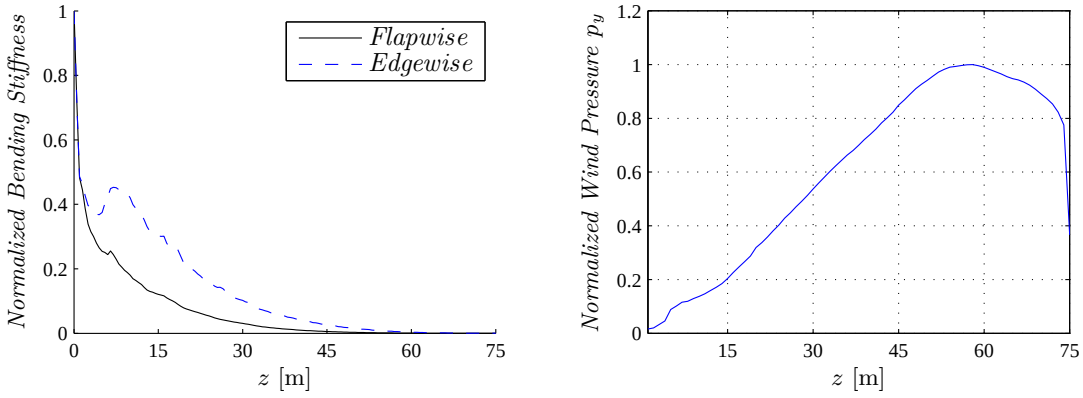

Fig. 9 a) Normalized flapwise and edgewise bending stiffnesses, b) Normalized wind pressure distribution at right angle to the plane of rotation.

The blade is loaded by the distributed force p_y, acting normal to the local secant direction. The

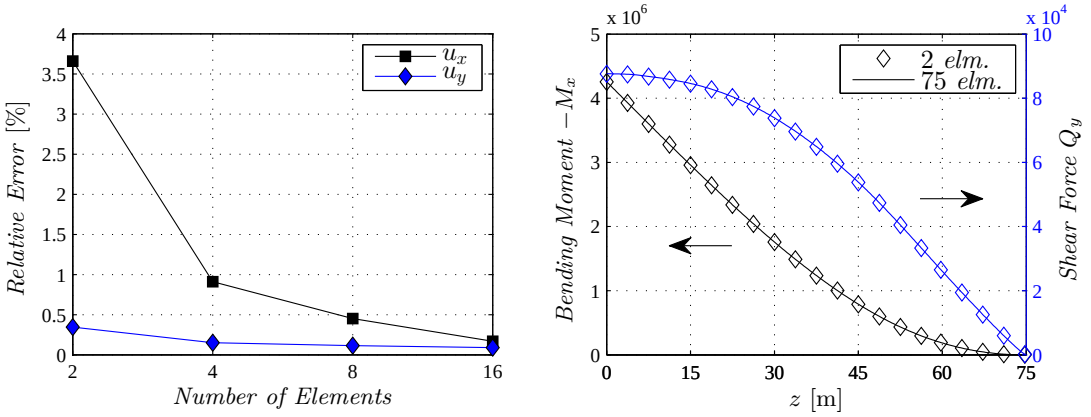

Fig. 10 Distributed lift force: a) Static tip deflection, b) Moment and shear force.

lengthwise distribution of the wind load p_y is shown in Fig. 9b. The linear increasing lift for the inner two-thirds of the blade that can be observed is a result of the blade's pre-twist. Furthermore, the reduction in aerodynamic load at the blade tip is attributed to tip losses. The deflection associated with this component of the wind pressure must be determined with high accuracy as it tends to bend the blade back against the tower. The relative error of the in-plane tip displacement obtained using the models with two, four, height, and sixteen elements relative to a reference deflection calculated using 75 elements under the wind pressure are shown in Fig. 10a. The elastic axis of the blade is not straight, and therefore four elements are required to determine both in-plane displacement components to within 1 % relative error. If the blade was straight, the quasi-static deflection under a tip load could be calculated exactly using a single element.

The distributions of the internal shear force Q_y and the moment M_x recovered using the present equilibrium method are shown in Fig. 10b for 2 and 75 elements. Naturally, they are identical apart from numerical rounding errors, but the curves illustrate the variation needed to be represented inside the large element to obtain full accuracy without additional nodes.

VI. Conclusions

A complementary energy formulation has been presented for a two-node straight beam element in which the stiffness matrix and the representation of distributed loads are calculated from equilibrium internal force distributions without any need for shape functions. The three main features are that the formulation permits: i) arbitrary lengthwise variation of the cross-section properties by in-

tegrating local cross-section flexibility weighted with simple and known internal force distributions, ii) representation of arbitrary cross-sections with coupled properties, e.g. from material anisotropy, represented by a full six by six local flexibility matrix, and iii) an exact formula for the equivalent nodal loads for arbitrary distributed loads, represented via equilibrium internal forces. The formulation includes the effect of shear flexibility directly via the additive flexibility format. The element stiffness properties determine the distribution of internal element loads to the equivalent concentrated loads at the element nodes, and it has been demonstrated that the correct evaluation of the equivalent nodal loads is essential for retaining the accuracy, when considering beams with large stiffness variations.

In principle the theory is exact as it is expressed in terms of integrals of the cross-section flexibility matrix and internal force distributions. The accuracy is only limited by approximations that may be involved in the evaluation of these integrals. However, as the functions to be integrated are available, in contrast to assumed shape functions, the accuracy of the evaluation is mainly a question of feasibility, and the final accuracy of the analysis is not directly related to the size of the elements. The use of equilibrium internal force distributions limits the full accuracy of the formulation to static problems. However, in most dynamics problems the local displacements due to element deformation are quite limited and the convected motion of the element dominates. This permits to retain a considerable part of the accuracy of the equilibrium based element stiffness formulation, also in dynamics problems when combined with the classic displacement based mass matrix. Additional accuracy of the representation of the mass matrix can be obtained by introducing extra internal degrees of freedom in the shape functions, and determining these additional parameters by fitting the corresponding displacement based stiffness matrix to that of the equilibrium based formulation described here.

Acknowledgment

The present paper is an extension of an unpublished internal note from 2006 describing the element stiffness matrix of a fully coupled nonhomogeneous beam without distributed loads. The present work has been supported by Siemens Wind Power A/S.

References

[1] Washizu K. *Variational Methods in Elasticity and Plasticity*, Pergamon Press, Oxford, 1974.

[2] Livesley RK. *Matrix Methods in Structural Analysis*, Pergamon Press, Oxford, 1975.

[3] Friedman Z, Kosmatka JB. Exact stiffness matrix of a nonuniform beam – I. Extension, torsion and bending of a Bernoulli-Euler beam. *Computers and Structures*, **42**, 671–682, 1992.

[4] Friedman Z, Kosmatka JB. Exact stiffness matrix of a nonuniform beam – II. Bending of a Timoshenko beam. *Computers and Structures*, **49**, 545–555, 1993.

[5] Krenk S. A general format for curved and non-homogeneous beam elements. *Computers and Structures*, **50**, 449–454, 1994.

[6] Molari L, Ubertini F. A flexibility-based finite element for linear analysis of arbitrarily curved arches. *Computers and Structures*, **65**, 1333–1353, 2006.

[7] Failla G, Impollonia N. General finite element description for non-uniform and discontinuous beam elements. *Archives of Applied Mechanics*, **82**, 43âĂŞ-67, 2012.

[8] Krenk S. *Non-linear Modeling and Analysis of Solids and Structures*, Cambridge University Press, Cambridge, 2009.

[9] Høgsberg J, Krenk S. Analysis of moderately thin-walled beam cross-sections by cubic isoparametric elements, *Computers and Structures*, **134**, 88–101, 2014.

[10] Cesnik CES, Hodges DH. VABS, A new concept for composite rotor blade cross-sectional modeling. *Journal of the American Helicopter Society*, **42**, 27–38, 1997.

[11] Hodges DH, *Nonlinear Composite Beam Theory*, Progress in Astronautics and Aeronautics, AIAA, Virginia, 2006.

[12] Yu W, Hodges DH, Ho JC. Variational asymptotic beam sectional analysis – An updated version. *International Journal of Engineering Science*, **59**, 40–64, 2012.

[13] Giavotto V, Borri M, Mantegazza P, Ghiringhelli G, Carmaschi V, Maffioli GC, Mussi F. Anisotropic beam theory and applications", *Computers and Structures*, **16**, 403–413, 1983.

[14] Ghiringhelli GL, Mantegazza P, Linear, straight and untwisted anisotropic beam section properties from solid finite elements, *Composites Engineering*, **4**, 1225–1239, 1994.

[15] Morandini M, Chierichetti M, Mantegazza P. Characteristic behavior of prismatic anisotropic beam via generalized eigenvectors, *International Journal of Solids and Structures*, **47**, 1327–1337, 2010.

[16] Bauchau OA, Han S. Three-dimensional beam theory for flexible multibody dynamics, *Journal of Computational and Nonlinear Dynamics*, **9**, 041011-1–12, 2014.

[17] Jonnalagadda Y, Whitcomb JD. Calculation of effective section properties for wind turbine blades, *Wind Energy*, **17**, 297–316, 2012.

[18] Couturier PJ, Krenk S, Høgsberg J, Beam section stiffness properties using a single layer of 3D solid elements, *Computers and Structures*, **156**, 122–133, 2015.

[19] Krenk S, Høgsberg J, *Statics and Mechanics of Structures*, Springer, Dordrecht, 2013.

[20] Chandra R, Stemple AD, Chopra I. Thin-walled composite beams under bending, torsional, and extensional loads, *Journal of Aircraft*, **27**, 619–626, 1990.

[21] Smith EC, Chopra I. Formulation and evaluation of an analytical model for composite box-beams,

Journal of the American Helicopter Society, **36**, 23–35, 1991.

[22] Stemple AD, Lee SW. Finite-element model for composite beams with arbitrary cross-sectional warping, *AIAA Journal*, **26**, 1512–1520, 1988.

[23] Ghiringhelli GL. On the linear three-dimensional behaviour of composite beams, *Composites Part B: Engineering*, **28**, 613–626, 1997.